ESTIMATION OF ROOT DIAMETER IN GPR IMAGES VIA CYCLEGAN-GUIDED MULTI-OBJECTIVE INTEGRATION NEURAL NETWORK

Xihong Cui, Shupeng Li, Luyun Zhang

State Key Laboratory of Remote Sensing Science, Faculty of Geographical Science, Institute of Remote Sensing Science and Engineering, Beijing Normal University

ABSTRACT

The diameter of roots is crucial to study the geometric characteristics of subsurface root structure. Due to the invisibility of the underground root system, its diameter parameters are also difficult to obtain directly. Therefore, estimating the diameter based on ground-penetrating radar B-Scan images is challenging. In this study, CycleGAN-guided multi-objective integration neural network (CMI-Net) was constructed to simultaneously extract root diameter and location. The CMI-Net includes two sub-networks: CycleGAN and YOLOv4-Hyperbolic Position and Diameter (YOLOv4-HPD). The former ensures that the YOLOv4-HPD model, trained on the simulated datasets, can be used in the field environment. The latter can accurately identify the root objects and estimate the root diameter. The performance of the model was evaluated using simulated test dataset and field control experimental dataset. The model's availability in estimating root diameter was demonstrated by the experimental results.

Index Terms— Root diameter estimation, CycleGAN, YOLOv4-HPD, GPR

1. INTRODUCTION

Plant roots can improve their adaptability to the subsurface soil environment by adjusting root size, root biomass, and root length [1]. Root diameter, among these factors, is crucial for studying the geometric characteristics of subsurface root structure [2]. However, obtaining root diameter information under field conditions is difficult because field investigations are often destructive, laborious, and time-consuming [3]. Ground Penetrating Radar (GPR) has been successfully used as a tool for nondestructive detection of plant roots to estimate root diameter parameters [4].

Previous studies merged the raw GPR data into a mathematical model of hyperbolic reflections and then calculated the relevant parameters based on the fitted hyperbola [5, 6]. However, the shape of the hyperbola is not sensitive to the diameter information, and it is not easy to estimate the diameter of the subsurface root by hyperbola fitting with high accuracy. *Hao Liang et al.* reported that the prediction results of the BP neural network model were more stable compared to the least squares regression model [7]. However, the method is based entirely on simulated experiments, which require further experiments using inhomogeneous roots and soils, and the actual dielectric constants of roots and soils are not readily available for practical field applications.

The CycleGAN-guided multi-objective integrated neural network (CMI-Net) model is proposed in this study to extract root information features from simulated GPR images and establish their relationship with root diameter, eventually being able to estimate both the precise location and diameter of root objects simultaneously on a given real-world GPR image.

2. MATERIALS AND METHODS

2.1. CMI-Net Model

The overall network structure of CMI-Net model is shown in Fig. 1 and consists of two sub-networks: one is the CycleGAN, which is used for domain migration to generate the diameter training dataset of roots with complex background in the field; The other one is the YOLOv4-HPD (YOLOv4-Hyperbolic Position and Diameter) model, which is proposed on the basis of YOLOv4 and improved for the YOLOv4-Hyperbola model by further expanding the prediction head so that it can estimate the diameter parameter simultaneously on the foundation of the predicted position.
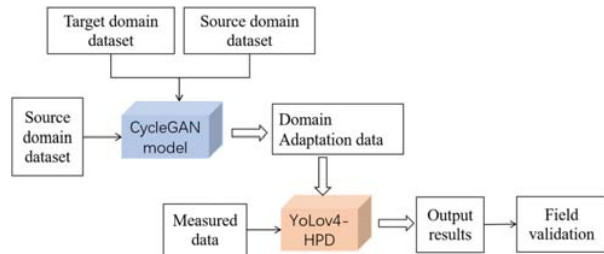
Fig. 1. The overall framework of CMI-Net

The CycleGAN is a ring network formed by two mirror-symmetric Generative Adversarial Network (GAN) with two generators and two discriminators, divided into forward network (source domain X to target domain Y) and reverse network (target domain Y to source domain X) [9]. In this study, a large number of real root diameter training dataset is not available, but a large number of real root dataset with unknown diameter information and simulated root dataset with known attribute information are available. The domain adaptation model is just right for the purpose of training on the simulated data and then applying it to the measured data.

The YOLOv4-HPD is a network used to extract the location and diameter parameters of the root target based on YOLOv4-Hyperbola [8], as shown in Fig. 2. YOLOv4-HPD adds a diameter prediction branch to YOLOv4-Hyperbola and redesigns the loss function. The output dimension of YOLOv4-HPD becomes 17-D, which includes the location information of the root (detection box, hyperbolic vertex, and four hyperbolic tail points) and the attribute information of the root (diameter).
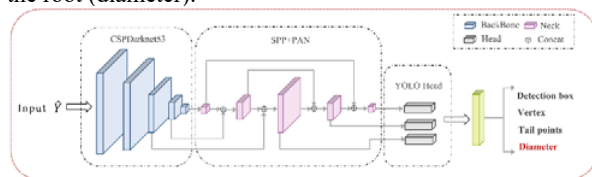
Fig. 2. YOLOv4-HPD network structure

2.2. Data Description

2.2.1. Field Datasets

The root diameter validation dataset was collected from a single root burial control experiment conducted in the same study area. A sample of shrub roots of different diameters, relatively straight and of uniform length, was selected as shown in Fig. 3b. Tow sand trenches were excavated in a flat clearing, each with a length of 3 m and a depth of 0.5 m. The holes were drilled in the trench wall on one side of the vertical sand trench. Six coarse shrub roots were inserted and a hollow was left. Considering the effect of root signal on the image, the experiment was divided into two groups, the first group of root samples was perpendicular to the horizontal ground, and the second group of root samples was at an angle of 30° from the ground. The depth of root samples in the first group was 0.3 m, and in the second group was 0.2 m. The spacing between roots was 0.4 m. After the root samples were inserted (as shown in Fig. 3a), the excavated soil was refilled and the clearing was releveled. The portable GPR system then detected the buried root samples in the subsurface following a preset measuring line (horizontal angle of 90° between the measuring line and the root samples). There were two experimental sand trenches, so four GPR images containing the reflected signals from the root samples were used for model validation. For the GPR images obtained for root detection in the field, the steps of data preprocessing include *detrending*, *dewow filtering*, *background removal*, and

amplitude gain [10], these operations are realized by MATGPR software [11].
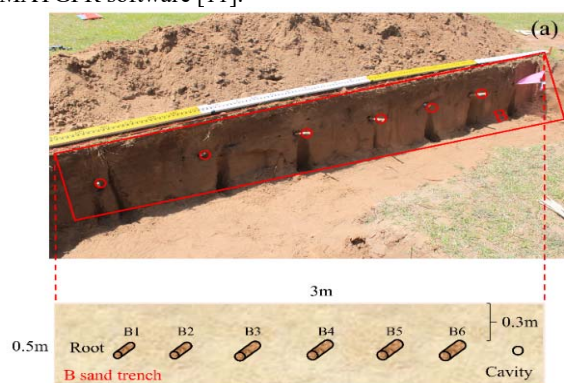
Fig. 3. Schematic of the control experimental design.

2.2.2. Synthetic Datasets

The GprMax V2.0 [12] was used to generate simulated dataset of root samples with different diameters for training. In this experiment, the size of the geometric domain was set to 1.8 m×0.5 m and the center frequency of GPR was still set to 900 MHz. The diameters of roots were set to 6 gradients, 10 mm, 14 mm, 18 mm, 22 mm, 26 mm, 30 mm. The dielectric constants of roots and soil were set in three groups in the experiment where the dielectric constants of roots were 9.21, 12.01, and 14.81, and the dielectric constants of soil were 3.70, 4.90, and 6.50. They were combined two by two to produce nine sets of dielectric constant differences.
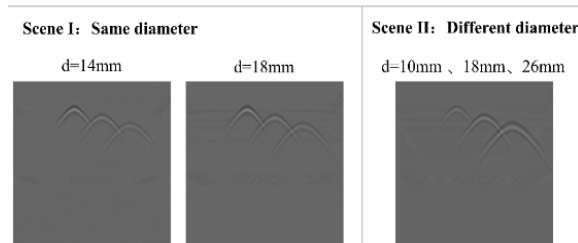
Fig. 4. Examples of different root GPR images in two simulated scenarios

To enhance the model's learning of the root object's diameter information in GPR images, simulation scenarios are divided into two categories (as shown in Fig. 4): Class I is the same diameter roots placed at different horizontal positions and different depths, and the soil dielectric constant and root dielectric constant are varied in turn to obtain six sets of simulation data; Class II is the different diameter roots placed at different horizontal positions and different depths, and the soil dielectric constant and root dielectric constant are changed in turn to obtain two sets of simulation data. Each group simulated 450 images, and a total of 3600 simulated GPR root images with different attribute information were obtained as training data for the domain adaptation model.

2.3. Experimental Setup and Evaluation Metrics

The CMI-Net model experiment setting is generally divided into two parts. Firstly, the experimental setup of CycleGAN is introduced. A total of 2418 images acquired from simulation and field experiments, were chosen as the source domain dataset and target domain dataset, respectively. The ratio of training, and test datasets is 1:1The batch size is 2, the initial learning rate is set to 0.0002, and a total of 100 epochs are trained. Secondly, the experimental setup of YOLOv4-HPD is introduced. A total of 3600 generator-generated image were used. The ratio of training, validation, and test datasets is 7:2:1. The batch size was 6, the initial learning rate was set to 0.01, and a total of 200 epochs were trained.

3. RESULTS AND DISCUSSION

3.1. Results of Domain Adaptation

Different simulated images will generate different real-word background images under different weight parameters. In order to make the YOLOv4-HPD model better applied to field measured data, this study uses simulated data as much as possible to generate sample images similar to the real situation. As shown in Fig. 5, a1-e1 are simulated GPR images of roots with different depths, horizontal positions, dielectric constants, and diameters, and a2-e2 are samples with different backgrounds generated by the trained CycleGAN model.
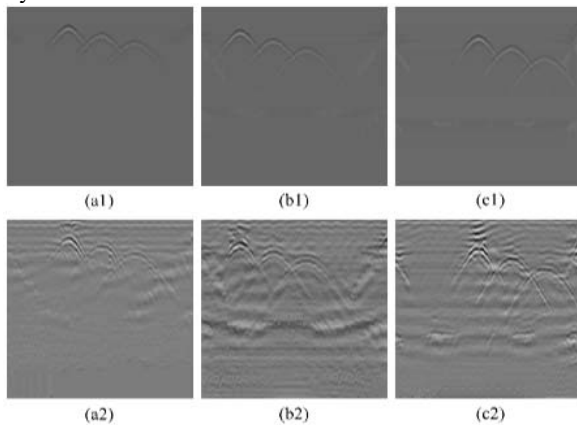
Fig. 5. (a1)-(c1) Original simulation images. (a2)-(c2) Domain migration results.

The results show that the shape and opening size of the hyperbolic signal are well preserved and successfully converted from a homogeneous background to a non-homogeneous background similar to the measured image. The brightness and texture of the images are greatly improved. It can be seen that the trained CycleGAN model can generate high-quality domain migration images and achieve more realistic style migration effects.

3.2. Results of Root Diameter Estimation

The YOLOv4-HPD model was trained with 200 epochs, and 360 images were used for model testing, including 270 images of scenario I and 90 images of scenario II. The trained YOLOv4-HPD model localized root objects on 360 test images while estimating root diameter parameter. The object detection evaluation indexes Precision, Recall, F1, and APIoU=0.5 and the keypoint evaluation index APoks=0.5 [13] all reached above 0.95 on the test dataset. Fig. 6 shows the detection results using YOLOv4-HPD on the test dataset. Figs. 6a-f is the image in scenario I, and the real root diameters on the image are 10 mm, 14 mm, 18 mm, 22 mm, 26 mm and 30 mm respectively. Figs. 6g-h is the image in scenario II, and the root diameters from left to right in Fig. 6g are 10 mm, 18 mm and 26 mm respectively, and the root diameters from left to right in Fig. 6h are 14 mm, 22 mm and 30 mm respectively. It can be seen that YOLOv4-HPD can not only accurately identify and locate each hyperbola, but also accurately extract root diameter parameters at different depths, with the error of about 1 mm.
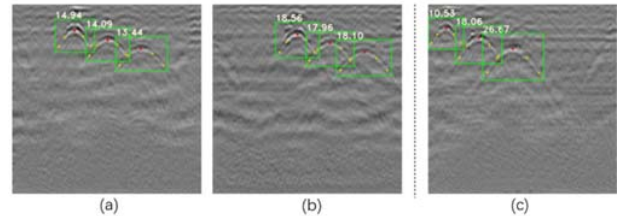
Fig. 6. (a)-(b) Image detection results of scenario I. (c)Image detection results of scenario II.

3.3. Model Generalization Verification

The measured data from control experiment are used to validate the generalization performance of the YOLOv4-HPD model trained on a pseudo-target domain dataset (Y´) (Fig. 7). As shown in Fig. 7, a total of 19 root signals were presented on the GPR images and 56% of the measured root samples had absolute diameter errors of less than 2 mm. More than half of the root samples had a relative error of less than 15% in diameter estimation. The YOLOv4-HPD, which is not trained on the measured data set, is still applicable on the measured data and can achieve high accuracy in locating and predicting the root diameter, and it has strong transferability.

4. DISCUSSION

Traditionally, the root diameter is estimated by constructing an empirical relationship between the root diameter and the amplitude or waveform parameters of the radar reflected signal [14, 15]. For example, Cui et al.(2010) utilized the electromagnetic waveform parameter (ΔT) manually extracted from the A-Scan data measured by GPR as an independent variable to build a linear regression model

6478

to estimate the root diameter. The RMSE of the regression model on the validation data is 3.53 mm. Whereas the maximum RMSE of the root diameter extracted by the CMT-Net model developed in this study is 1.72mm on the test data, and the RMSE estimated for the measured root sample diameter is only 3.30mm (Fig.7). Compared with the traditional method, the accuracy of the root diameter estimation has significantly improved. The construction process of these traditional methods varies depending on the study area and soil background, and the radar reflection signal parameters utilized are also different, resulting in a lack of a unified method and process for data pre-processing and root diameter extraction. The extraction of radar reflection signal parameters mostly relies on manual interpretation, which is subjective and needs to be further adjusted and tested in practical application. However, the CMT-Net model developed in this study can overcome these problems.
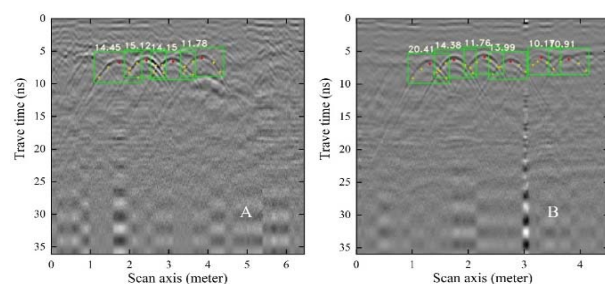
Fig. 7. Detection results of YOLOv4-HPD on real dataset

5. CONCLUSION

In this study, A novel deep learning model, CMI-Net, for root object localization and root diameter extraction on GPR B-Scan images was constructed using measured data collected by a GPR system with 900 MHz antenna and simulated data generated by GprMax V2.0. The CMI-Net model was effectively validated on both simulated and measured data. The hyperbolic signals reflected from all root samples on the measured data were correctly located, and the root diameter estimation results showed that 56% of the root samples had absolute root diameter errors within 2 mm. These results all indicate the applicability of the CMI-Net model for accurately locating root locations and estimating root diameter parameters in field experiments. This method helps to reconstruct the three-dimensional structure of the below-ground root system, which in turn helps to analyze the correlation between above-ground and below-ground characteristics of plants at the regional scale.

5. REFERENCES

[1] R. A. GILL and R. B. JACKSON, "Global patterns of root turnover for terrestrial ecosystems," *New Phytol.,* vol. 147, no. 1, pp. 13-31, July 2000.

[2] Y. Keitaro *et al.*, "Ground-penetrating radar estimates of tree root diameter and distribution under field conditions," *Trees,* vol. 32, pp. 1657-1668, August 2018.

[3] X. H. Cui, L. Guo, J. Chen, X. H. Chen, and X. L. Zhu, "Estimating tree-root biomass in different depths using ground-penetrating radar: Evidence from a controlled experiment," (in English), *IEEE Trans Geosci Remote Sens,* vol. 51, no. 6, pp. 3410-3423, Jun 2013, doi: 10.1109/Tgrs.2012.2224351.

[4] C. V. M. Barton and K. D. Montagu, "Detection of tree roots and determination of root diameters by ground penetrating radar under optimal conditions," *Tree Physiol.,* vol. 24, no. 12, pp. 1323-31, Dec 2004, doi: 10.1093/treephys/24.12.1323.

[5] A. V. Ristic, D. Petrovacki, and M. Govedarica, "A new method to simultaneously estimate the radius of a cylindrical object and the wave propagation velocity from GPR data," *Computers & Geosciences,* vol. 35, no. 8, pp. 1620-1630, 2009.

[6] L. Chen, Y. Wang, C. Ren, B. Zhang, and Z. Wang, "Optimal combination of predictors and algorithms for forest above-ground biomass mapping from Sentinel and SRTM data," (in English), *Remote sensing (Basel, Switzerland),* vol. 11, no. 4, p. 414, Feb 2 2019, doi: 10.3390/rs11040414.

[7] H. Liang, G. Q. Fan, Y. H. Li, and Y. D. Zhao, "Theoretical Development of Plant Root Diameter Estimation Based on GprMax Data and Neural Network Modelling," (in English), *Forests,* Article vol. 12, no. 5, p. 22, May 2021, Art no. 615, doi: 10.3390/f12050615.

[8] S. P. Li, X. H. Cui, L. Guo, L. Y. Zhang, X. H. Chen, and X. Cao, "Enhanced automatic root recognition and localization in GPR images through a yolov4-based deep learning approach," (in English), *IEEE Trans Geosci Remote Sens,* Article vol. 60, p. 14, 2022, Art no. 5114314, doi: 10.1109/tgrs.2022.3181202.

[9] J. Y. Zhu, T. Park, P. Isola, and A. A. Efros, "Unpaired Image-to-Image Translation using Cycle-Consistent Adversarial Networks," in *Proceedings of the IEEE International Conference on Computer Vision (ICCV)*, 2017, pp. 2223-2232.

[10] X. H. Cui *et al.*, "The root-soil water relationship is spatially anisotropic in shrub-encroached grassland in north China: Evidence from GPR investigation," (in English), *Remote Sens,* vol. 13, no. 6, Mar 2021, doi: 10.3390/rs13061137.

[11] A. Tzanis, "matGPR Release 2: A freeware MATLAB package for the analysis & interpretation of common and single offset GPR data," vol. 15, no. 1, pp. 17-43, 2010.

[12] A. Giannopoulos, "Modelling ground penetrating radar by GprMax," *Construction & Building Materials,* vol. 19, no. 10, pp. 755-762, 2005.

[13] J. R. Butnor, J. A. Doolittle, L. Kress, S. Cohen, and K. H. Johnsen, "Use of Ground-Penetrating Radar to study tree roots in the southeastern United States," *Tree Physiol.,* vol. 21, no. 17, pp. 1269-78, Nov 2001, doi: 10.1093/treephys/21.17.1269.

[14] X. Cui, J. Chen, J. Shen, X. Cao, X. Chen, and X. Zhu, "Modeling tree root diameter and biomass by ground-penetrating radar," Science China Earth Sciences, vol. 54, no. 5, p. 711, 2011.

[15] H. Liang, G. Fan, Y. Li, and Y. Zhao, "Theoretical Development of Plant Root Diameter Estimation Based on GprMax Data and Neural Network Modelling," Forests, vol. 12, no. 5, p. 615, 2021.